Eur. Phys. J. B **34**, 119–129 (2003)
DOI: 10.1140/epjb/e2003-00203-7

THE EUROPEAN PHYSICAL JOURNAL B

On the aging dynamics in an immune network model

M. Copelli[1,a], R.M. Zorzenon dos Santos[1], and D.A. Stariolo[2,b]

[1] Laboratório de Física Teórica e Computacional, Departamento de Física, Universidade Federal de Pernambuco, Cidade Universitária, 50670-901, Recife, PE, Brazil
[2] Instituto de Física, Universidade Federal do Rio Grande do Sul, CP 15051, 91501-970, Porto Alegre, RS, Brazil

Received 8 February 2003 / Received in final form 7 May 2003
Published online 23 July 2003 –

Abstract. Recently we have used a cellular automata model which describes the dynamics of a multi-connected network to reproduce the refractory behavior and aging effects obtained in immunization experiments performed with mice when subjected to multiple perturbations. In this paper we investigate the similarities between the aging dynamics observed in this multi-connected network and the one observed in glassy systems, by using the usual tools applied to analyze the latter. An interesting feature we show here, is that the model reproduces the biological aspects observed in the experiments *during* the long transient time it takes to reach the stationary state. Depending on the initial conditions, and without any perturbation, the system may reach one of a family of long-period attractors. The perturbations may drive the system from its natural attractor to other attractors of the same family. We discuss the different roles played by the small random perturbations ("noise") and by the large periodic perturbations ("immunizations").

PACS. 87.18.Hf Spatiotemporal pattern formation in cellular populations – 87.10.+e General theory and mathematical aspects – 61.43.Fs Glasses

1 Introduction

In this paper we discuss a model for the evolution of the immune repertoire of B cells, which are responsible for the humoral immune responses. B cells belong to one of the main classes of white blood cells: the lymphocytes. These cells carry on their surface the order of 10^5 molecular receptors (proteins) and once activated they produce antibodies, which are copies of their molecular receptor. During the life time of an individual the immune system is able to produce the order of 10^{11} different antibodies or different populations of B cells. The antigen (virus, bacteria, poison, cellular residue, etc.) is not recognized as a whole but by its epitopes, which are patches on its structure that may be recognized by specific sites of the antibody molecules. By pattern recognition different antibodies will mark the epitopes of a given antigen, therefore forming a complex that will be eliminated by macrophages (another class of white blood cells) [1,2].

According to clonal selection theory [1,2], elements that challenge the immune system will determine the populations (clones) of B cells that will proliferate: those populations will produce antibodies which will be able to recognize different epitopes of the specific antigen. The immune network theory [2,3], however, is based on the fact that the antibodies (and molecular receptors) are able to recognize and to be recognized, and therefore during the immune response there are different types of interaction: antigen-antibodies and antibodies-B cells. In other words, when a given population of B cells is activated by the presence of a given antigen the produced antibodies will not only mark the specific antigens but also activate new B cell populations with complementary molecular receptors, which in turn will recognize them. The increase on the concentration of these complementary populations, on their turn, will maintain the proliferation of the antigen recognizing population, installing a feedback mechanism that will keep several populations activated. This kind of dynamics will generate a functional multi-connected network among different populations of B cells that will be dynamically regulated by mechanisms of activation and suppression. The network will then play an important role on the regulation of the immune responses. Although the immune network theory is part of the current immunological thinking, there are only few experiments supporting the interaction among clones with complementary receptors and the existence of such a network [4,5]. According to these experimental findings, if the network exists only $10-20\%$ of the populations will belong to it, the rest of the immunocompetent populations remaining at rest.

Recently we have successfully used a mathematical model [6–8,16] (inspired in a previous one proposed by de Boer *et al.* [17]) which takes into account the main

[a] e-mail: mcopelli@df.ufpe.br
[b] Research Associate of the Abdus Salam International Center for Theoretical Physics, Strada Costiera 11, Trieste, Italy

features of Jerne's immune network theory, to simulate experiments on immunization and aging performed with mice [9] that could not be explained by the clonal selection theory. The simulations allowed to interpret the experimental results from the point of view of the immune network theory.

The model allows to follow the evolution of the concentrations of the different populations of B cells in discrete shape space, a formalism which maps all possible molecular receptors of a given organism into points of a d-dimensional space. To each point (receptor) we associate a clone that corresponds to the population of B cells and antibodies characterized by this molecular receptor. The concentration of each clone will be described by a three-state automaton representing low, medium and high concentrations, and the interaction among different clones is based on complementarity. As far as we know, the model [6,7,16,17,19] corresponds to the first successful attempt in describing the dynamics of the immune network as proposed by Jerne [3] and recently it could be used to reproduce experimental results performed with mice [9]. Besides the biological implications of the results obtained in reference [9], the dynamical behavior exhibited by this model in the biologically relevant parameter region is quite interesting by itself and should be better investigated. This region has been shown [6] to exist for dimensions $d \geq 2$ and comprises a broad stripe near the transition between stable and chaotic behaviors, in which the model describes a multi-connected functional network [6,7]. In this region we found the majority of the populations in the resting state (low concentration) while the activated ones may reach $10 - 20\%$ of the total number of populations. The activated populations are aggregated in clusters of different sizes, which fuse and split as time passes following an aggregation and disaggregation dynamics. Therefore the largest cluster at each time step is found in a different region [7].

In the experiments described in reference [9], 6 mice of the same linage are subjected to the immunization protocol as follows: the researchers inject ova by means of an intra-venal injection, wait for 14 days and measure the number of specific antibodies. Then they inject again the same amount of antigen, wait for 7 days and measure the amount of antibodies, and continue by repeating the same protocol every 7 days. In order to simulate the immunization protocol, the cellular automaton (CA) is subjected to specific perturbations by flipping chosen resting populations (low concentration) to their activated state (high concentration). Depending on the perturbation (damage) size, it may disappear after a few time steps or part of the damage (activated populations) may be incorporated to the network. In other words, the memory about the perturbations is due to the ability of the system to adapt (plasticity) and incorporate information about them. We have used two types of perturbations: random small ones, which correspond to the noise that mice are subjected to during the experiment, caused by the environment, and periodic large ones that will simulate the immunization protocol of multiple antigen perturbations under the same conditions [9]. After few presentations there is a saturation of the response of the system to the perturbation. During this process, the system incorporates new information and some of the previous information is lost, keeping the number of activated sites in the network almost unchanged. This kind of behavior was also observed experimentally in mice [10], where saturation is related to a refractory behavior of the immune system.

We have also observed aging effects on the dynamics of this system [9]. An older system is more rigid: the network loses plasticity to incorporate new information [9,11,12]. A recent study [13] has shown that the distribution of cluster sizes during the time evolution of the system has a characteristic cluster size (exponential behavior), but the distribution of persistence times (the period during which a given population remains activated and belongs to the network) exhibits a power law behavior. While the existence of a characteristic cluster size may be related to the loss of plasticity, the power law behavior of the persistence time may be associated to the memory generated by the dynamics of the system.

The question we address here refers to how the learning process takes place dynamically and what is the cause of the loss of plasticity. The slow dynamics observed in this system presents analogies with the physical aging effects observed and reported on glass studies [14,15]: as the system gets older (ages) there is a loss of plasticity for structural or molecular relaxation and less changes are observed during the relaxation time. The mechanisms underlying the slow dynamics of glassy systems are the spatial (or geometric) disorder related with the difficulty to satisfy simultaneously all microscopic interactions, a characteristic called *frustration*. Glasses and spin glasses exhibit a rough energy landscape with many local minima which is responsible for slowing down the relaxation towards equilibrium. Their dynamics depends on the past history of the sample and under small perturbations they relax slowly. In our biologically motivated model the nonlocal interactions are based on complementarity (both perfect and slightly defective matches) and reflect the activation and suppression mechanisms in the complementary regions of the shape space. The analogue to frustration, in the network, is generated by the inability of the system to incorporate information and to satisfy the constraints of the activation and suppression mechanisms. We show that the CA dynamics gives rise to a large family of periodic attractors which are very robust, and could be regarded as the analogues of the minima in the glassy systems. The loss of plasticity and aging effects will therefore be related to the non-ergodicity in the phase space.

In this paper the dynamics of the immunological responses in the network model are investigated using the common tools adopted in the study of glassy systems [15]. In particular we will focus on the relaxation of two-time autocorrelations of the B-cell populations, the structure of the attractors and effects of perturbations and immunizations. The paper is organized as follows: in Section 2 we describe the model and the procedures adopted in order to measure the correlations among different configurations

of the system; in Section 3 we present and discuss the results obtained for small and large perturbations and in Section 4 we present a summary, prospectives for future work and some conclusions.

2 The model

The model under study here is a modified version [6–8] of the model proposed by Stauffer and Weisbuch [16], which in turn was inspired in a previous model proposed by de Boer *et al.* [17] to describe the time evolution of the immune repertoire. It is a deterministic window cellular automaton model based on the shape space formalism [18], which describes the interactions of B-lymphocytes and antibodies, and the main mechanism underlying these interactions, which is pattern recognition (lock-key interaction). The dynamics of the system is regulated by specific interactions involving complementary molecular receptors of the different clones. The memory about the relevant antigens, presented to the system during its past history, emerges from the dynamics of the system, rather than being stored in a static registry.

To each point of a d-dimensional discrete lattice we associate a given receptor, which in turn will be described by d-coordinates representing important physical-chemical features of the receptor that differentiate one from the other [18]. Since clones are classified according to their molecular receptor, to each point $\vec{r}$ of the discrete shape space we associate a three-state automaton $B(\vec{r},t)$ that will describe the concentration of its population over the time: low ($B(\vec{r},t)=0$), intermediate ($B(\vec{r},t)=1$) and high ($B(\vec{r},t)=2$).

The time evolution of the cellular automaton is based in a non-local rule: population $B(\vec{r},t)$ at site $\vec{r}$ is influenced by the populations at site $-\vec{r}$ (its mirror image or complementary shape) and its nearest-neighbors ($-\vec{r}+\delta\vec{r}$) (representing defective lock-key interactions). The influence on the population at site $\vec{r}$ due to its complementary populations is described by the field $h(\vec{r},t)$:

$$h(\vec{r},t)=\sum_{\vec{r}\,'\in(-\vec{r}+\delta\vec{r})} B(\vec{r}\,',t) \qquad (1)$$

where for a given $\vec{r}$ the sum runs over the complementary shape $\vec{r}\,'=-\vec{r}$ and its nearest neighbors. Due to the finite number of states of the population B, the maximum value of the field $h(\vec{r})$ is $h_{max}=2(2d+1)$. The updating rule is based on a window of activation, which describes the dose response function involved in B-cell activation [6,16,17]. There is a minimum field necessary to activate the proliferation of the receptor populations (θ_1), but for high doses of activation (greater than θ_2) the proliferation is suppressed. The updating rule may be summarized as:

$$B(\vec{r},t+1)=\begin{cases} B(\vec{r},t)+1 & \text{if} \quad \theta_1\le h(\vec{r},t)\le\theta_2 \\ B(\vec{r},t)-1 & \text{otherwise} \end{cases} \qquad (2)$$

but no change is made if it would lead to $B=-1$ or $B=3$. We define the densities of sites in state i at time t as $B_i(t)$ ($i=1,\,2,\,3$).

The initial configurations are randomly generated according to the following concentrations: $B_1(0)=B_2(0)=x/2$, while the remaining $L^d(1-x)$ sites are initiated with $B(\vec{r},0)=0$. This model may exhibit stable or chaotic behaviors depending on the values of x, θ_1 and $\theta_2-\theta_1$. However it is on the transition region between the two behaviors that the model behaves like a multi-connected network [6].

In order to simulate the immunization protocol performed in the mice experiments we have followed the procedure which is described in reference [9] and summarized below. We have adopted the scale of 5 time steps corresponding to 1 day [9]. While the system evolves according to the deterministic dynamics (Eq. (2)), small and large perturbations can be produced, by setting the state of the chosen sites at $B(\vec{r},t)=2$.

Small perturbations

The small perturbations account for the immunological stimuli (noise) coming from the environment. The time interval between two consecutive small perturbations is a random number uniformly distributed between 1 and 100 time steps. Each perturbation corresponds to a random number of damages (from 1 to 3) introduced at regions of resting populations ($B=0$) which are randomly drawn (at every perturbation). The size of each damage may also vary randomly from 1 to 3 (onion-like) concentric layers around a central site (containing 7, 25 or 63 populations, respectively, in 3 dimensions).

Large perturbations

The large perturbations correspond to the immunization protocol which starts at a predetermined age of the mice. Like in the experiments, we stimulate the system periodically (every 35 steps $\simeq$ 1 week), and always in the same region (which is initially chosen at random but kept unchanged along the simulation). The damage size in this case corresponds to six layers (377 populations) around an specific site.

Previous results on this model have shown [9] that the response to the immunizations presents a strong dependence on the initial time ("age") at which the periodic protocol starts (fitting experimental data extremely well for mice whose immunization protocol started at different ages). This has led us to the conjecture that the dynamical behavior of the system might be at least qualitatively similar to that of some glassy systems, despite the non-Hamiltonian nature of the CA dynamics.

One of the quantities commonly used in the study of glassy systems is the two-time autocorrelation function between the system configurations at two given times t and t_w. A common experiment in glassy systems consists in preparing the system at a high temperature and suddenly making a quench to a low temperature. Then the system is allowed to relax up to a *waiting time* t_w, whose configuration is recorded. As the system continues to relax the autocorrelations between the instantaneous configurations at time $t>t_w$ and that at time t_w are computed.

The waiting time t_w is called the *age* of the system in the context of glassy systems. The monitoring of the two-time autocorrelations gives important insights on the relaxation process. The dynamics, whether stationary or not, can be readily recognized on the t_w dependence of the autocorrelations, since in a stationary process two-time quantities depend only on time differences. Consequently by plotting correlations as a function of time difference $t - t_w$ for different waiting times it is possible to distinguish between an essential out of equilibrium process from a stationary one. The aging processes observed in glassy systems are then related to the lack of temporal invariance [15].

Inspired on this approach, we will analyze the multiconnected network dynamics by defining and analyzing quantities analogous to the two-time autocorrelations for the CA:

$$C_{tot}(t, t_w) = \frac{1}{N} \sum_{\vec{r}}^{N} \delta \left(B(\vec{r}, t_w), B(\vec{r}, t) \right) \tag{3}$$

$$C_{22}(t, t_w) = \frac{1}{B_2(t_w) N} \sum_{\vec{r} | B(\vec{r}, t_w) = 2}^{N} \delta \left(B(\vec{r}, t), 2 \right), \tag{4}$$

where $N = L^d$ is the total number of populations in the system. C_{tot} and C_{22} amount to normalized proximities (using Hamming distance as a measure) and from now on will be referred to simply as correlation functions. These quantities will be analyzed for different protocols: without any perturbation, with small perturbations (noise) and with large perturbations (immunization protocol) in order to differentiate the effects of the different kinds of perturbations.

A complementary view of the long-term behavior of the system can be obtained by looking at the attractors to which the system evolves. In the present case it will consist mainly of cycles, which will be reflected by the periodicity of the correlations. For this purpose, we have obtained the return maps of the consecutive maxima of the correlation functions. Note that the period of the maxima thus obtained does not correspond to the period of the real system, which is at least twice as long [19].

3 Results

3.1 Without perturbations

In previous works [6,7,19] it has been shown that depending on the initial concentration x of active populations the system may exhibit periodic or chaotic behavior. Systems with low initial concentrations of active sites ($x < x_c$) evolve to either fixed points or orbits with short periods, while for $x > x_c$ chaotic attractors appear. However, the biologically relevant region is in the transition region between these two behaviors, where the system reaches one of several periodic orbits (as will be seen below) with a very long period and after a long transient. From now on, all the results have been obtained using the same parameters adopted in reference [9]: $d = 3$, $\theta_1 = h_{max}/3$, $\theta_2 = 2h_{max}/3$ and $x = 0.26$ (on the transition region).

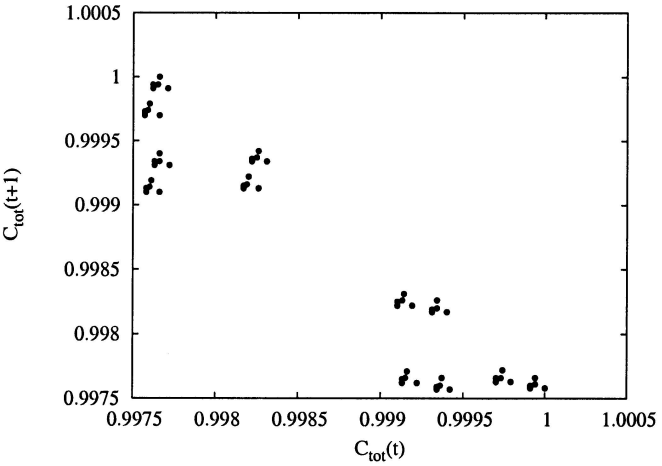

Fig. 1. Return map for maxima of the total correlation function $C_{tot}(t)$ for $L = 50$ and $t_w = 10\,000$ (single run).

Without any perturbation, the system evolves after a transient time towards a cycle with a large period, as shown in the return map of Figure 1. We have also varied the waiting time from 10 to 100 000 (not shown). The greater the waiting time, the closer to the attractor the system is, which is revealed by larger values of the autocorrelation functions. Once t_w is larger than the transient, the time series for $C_{tot}(t, t_w)$ (and also $C_{22}(t, t_w)$) will include unity (see Fig. 1) and will not change for larger values of t_w.

A typical result for the time evolution of the correlation functions for $t_w = 100$ is shown in Figure 2. The upper panel corresponds to the time evolution of the densities B_1 (intermediate concentrations) and B_2 (high concentrations), while the lower panel corresponds to $C_{tot}(t, t_w)$ (open circles) and $C_{22}(t, t_w)$ (filled circles). Notice that while the concentrations relax to approximately constant values in a short time, C_{tot} and C_{22} take much longer to reach their attractors (note the logarithmic time scale). In order to study how the system relaxes towards the attractor it is more convenient to make use of C_{22}, since it measures the changes in the (more relevant) network of activated populations. In the case shown in Figure 2 the transient time needed to attain the attractor is $\mathcal{O}(10^4)$ steps. It is necessary to point out, however, that this typical relaxation time is important only for the physical aspects of the dynamics. When mapped into the biological problem, it would correspond to $\sim$ 5.5 years, which is much longer than the average life time of the mice used in the kind of experiment we simulated. Therefore the relevant behavior, from the biological point of view, happens to be in the transient of the model and not in its stationary state, a result which is interesting on its own.

3.2 Random small perturbations

How does the behavior of the system change when random small perturbations are produced on the parameter region used to simulate the real experiments performed

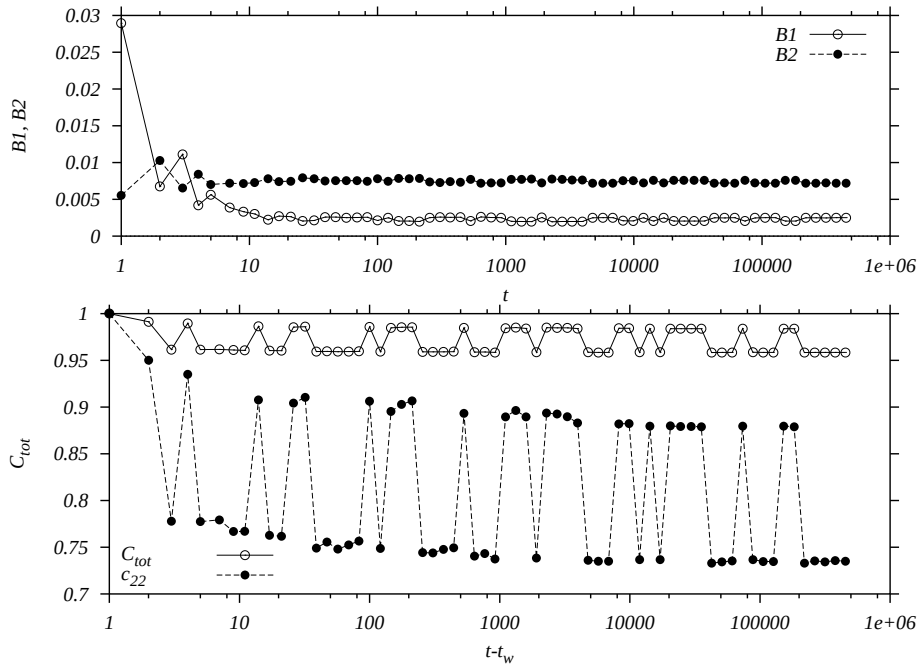

Fig. 2. Densities of intermediate and high concentrations *vs.* time (upper panel) and autocorrelations *vs.* $t - t_w$ for $L = 50$ and $t_w = 100$, without any perturbation.

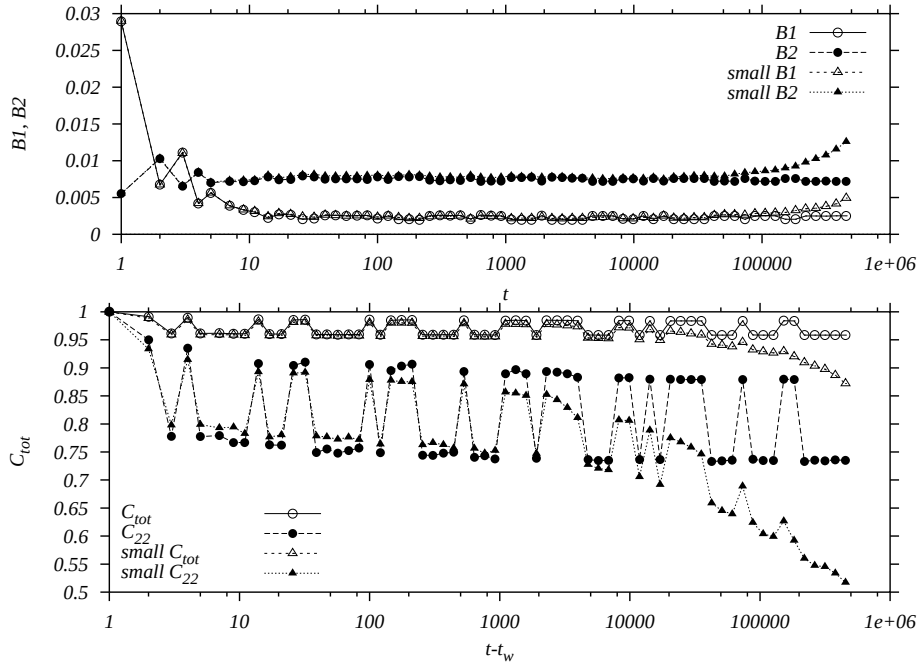

Fig. 3. Densities *vs.* time (upper panel) and correlations *vs.* $t - t_w$ for $L = 50$ and $t_w = 100$; without perturbation (circles) and with small perturbations (triangles).

with mice [9]? In order to investigate this issue, only the small perturbations described in Section 2 were produced, starting at time zero.

In Figure 3 we compare the time evolution of the densities and correlation functions obtained for single runs for the system without perturbations and with small random perturbations. Note that in the case with small perturbations the correlations initially follow those of the purely deterministic system, showing only small differences. After about $10^3 - 10^4$ steps, however, they start decreasing faster, indicating some sort of cumulative effect that drives the system away from the region in phase space that it had approached until t_w. These effects are more easily noted for C_{22}. Moreover, the perturbations do not alter the behavior of the densities, as expected, since the number of activated populations is kept approximately constant by

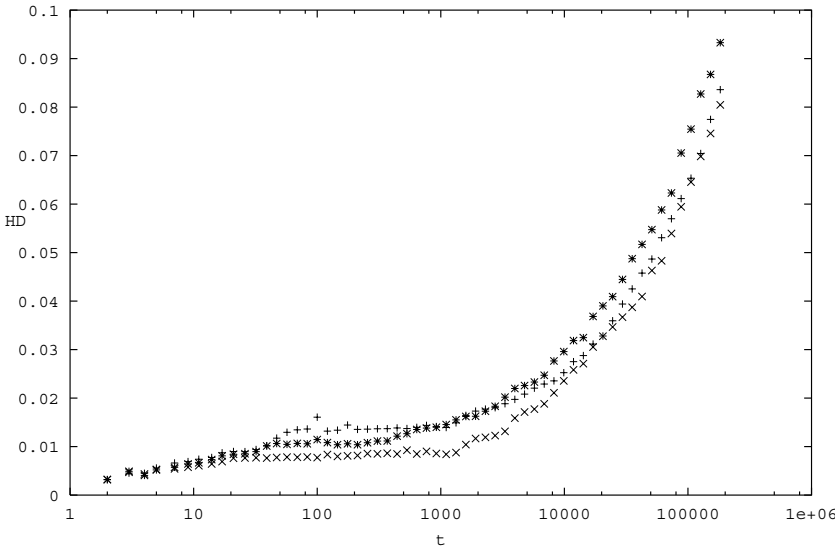

Fig. 4. Normalized Hamming distance between two initially identical configurations subjected to different sequences of small perturbations (three samples).

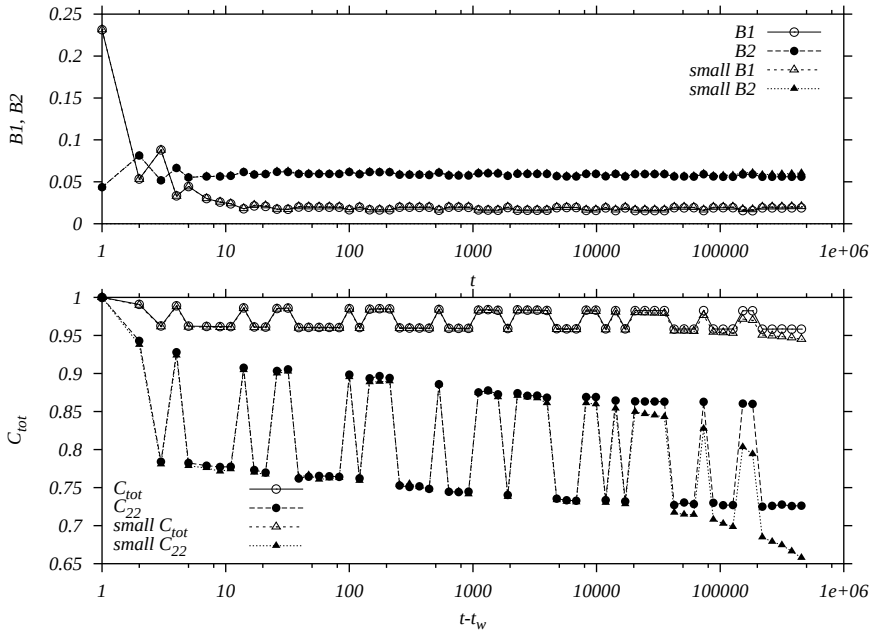

Fig. 5. Densities *vs.* time (upper panel) and autocorrelations vs. $t - t_w$ for $L = 100$ and $t_w = 100$ (the same conditions used in Fig. 3); without perturbation (circles) and with small perturbations (triangles).

the self-regulatory mechanisms embedded in the dynamical rules. The changes are observed only in the populations that belong to the active network: in order to incorporate new information (new populations), older ones are deactivated. From the biological point of view, the realizations of the perturbations (small and large) differ from one individual to another, building the identity of each individual. At the end of life each individual will have a different history in terms of perturbations (antigen presentations) translated into the configuration of the populations belonging to the active network. This is nicely illustrated by Figure 4, where two initially identical copies of a system undergo different realizations of the small perturbations according to the protocol described in Section 2. The Hamming distance between them grows on a long time scale, revealing the mechanisms behind the behavior of the correlations in Figure 3.

Returning to Figure 3, it is important to stress that the changes observed in the concentrations for very long times (upper panel) are due to finite size effects. They are caused by the fact that all small perturbations are produced on regions of resting populations. For a finite system, after a long time all the possibilities will have already been explored. Increasing the size of the system, the changes on the densities disappear. This is shown in Figure 5, where we repeat the simulations, under the same conditions of Figure 3, for a larger system ($L = 100$).

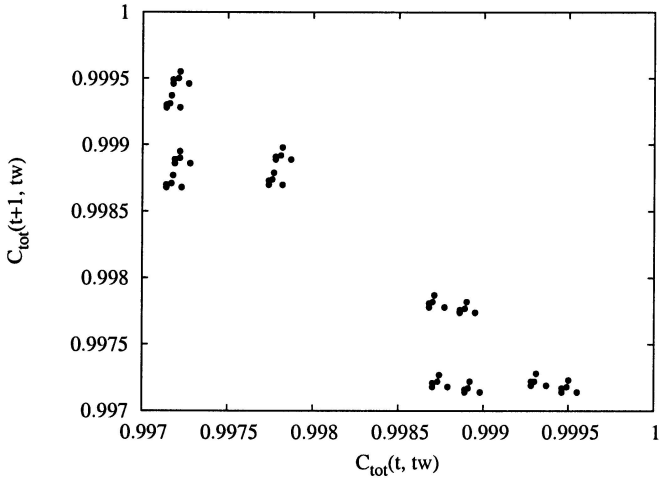

Fig. 6. Return map for maxima of total correlation function, for $L = 50$, $t_w = 10\,000$, $\Delta t_1 = 1000$ and $\Delta t_2 = 10\,000$.

In order to test out the robustness of these results, we have varied the parameters controlling the protocol of the random small perturbations. For instance, by increasing the maximum number of different perturbations from 3 to 6 at each presentation, and/or by changing the maximum time interval between consecutive perturbations from 100 to 10, we observe the same qualitative behavior, with a faster decrease of the correlations — as expected, since in both cases the noise has been increased.

What happens when the system's autocorrelations decrease due to the small random perturbations after it has reached a periodic attractor? Is the system driven to another cycle? To answer this question we have studied the stability of the cycles using the following procedure: we let the system evolve without perturbation towards its attractor for $t_w = 10\,000$ time steps, after which we perturb the system with random small perturbations during a time interval Δt_1. Then we turn off the perturbations and allow the system to relax during another time interval Δt_2 after which we obtain the return map of the correlations in the following 200 time steps. If we produce only one perturbation at t_w ($\Delta t_1 = 1$) the system remains in its original cycle, yielding a return map similar to that of Figure 1. Then, under the same conditions we repeat the simulations adopting now $\Delta t_1 = 1000$ and $\Delta t_2 = 10\,000$. We observe in Figure 6 that the return map has changed slightly when compared to Figure 1. In particular, it no longer shows $C_{tot} = 1$ in the time series, but remains periodic, signaling that the system has shifted to a different cycle due to the perturbations. Apparently the periods observed in Figures 1 and 6 are the same. The distribution of periods and transient times are currently under investigation, results will be published elsewhere. Figure 6 remains the same by increasing Δt_2, which guarantees that the differences with respect to Figure 1 are not a transient effect.

According to these results, the role the noise plays, if allowed enough time to perturb the system significantly, is to drive the system from one attractor to a nearby one, which suggests that there is a family of periodic attractors which can be very close to one another in phase space. These effects, however, take place on a time scale which is longer [$\mathcal{O}(10^3 - 10^4)$ time steps] than the lifetime of the mice [$\mathcal{O}(10^2 - 10^3)$ time steps]. The small perturbations are therefore of little importance to the CA dynamics in the biologically relevant time scale, as suggested in previous work [9].

The behavior of the autocorrelation functions in Figures 3 and 5 is reminiscent of what is observed in glassy systems. Here the CA approaches a periodic attractor, being thereafter deflected by the small perturbations. In glassy systems, temperature drives the system from one local minimum to another, preventing it from getting stuck in local minima of the potential energy surface. As the *physical age* of the system (characterized by the value of the waiting time t_w) grows, it finds itself exploring deeper and deeper regions of a rough potential energy surface, diffusing towards equilibrium [20]. Due to the roughness of the potential energy, equilibrium is only attained on very long time scales and relaxation is very slow. The older the system is the more it gets confined to a restricted region of phase space and the time scales for relaxation get longer and longer. Eventually, if we wait long enough, the system equilibrates and the dynamics becomes stationary, losing sensitivity to the waiting time. This picture of an aging physical system is reminiscent to the loss of plasticity for adaptation in a living organism as it gets older. In either case, one observes a strong dependence on the waiting time t_w, evident when measuring two-time quantities like autocorrelation functions and responses. Results for the CA model are shown in Figure 7, where we see the decay of autocorrelations for three systems with different *ages* or waiting times. Note that the horizontal axis is the time difference between the total time and the waiting time. The three curves should collapse in the case that the dynamical evolution is stationary.

3.3 Large immunizations

What is the role of the large perturbations on the dynamics of the system? From previous studies we would expect the large perturbations to accelerate the aging process: while the random small perturbations would change the route to the natural attractor of the system, the large ones would reduce the transient time, a conjecture that would explain the loss of plasticity of the older mice [9]. The protocol adopted is the one described in Section 2, with six-layer perturbations every 35 time steps, always at the same sites.

In Figure 8 we compare the results obtained for the unperturbed system and those of the system subjected only to large immunizations starting at t_w (note that the densities are now also plotted as functions of $t - t_w$). Somewhat surprisingly, the decrease of the correlations for large perturbations is small, when compared to the case of the small perturbations (compare with Fig. 3). In hindsight,

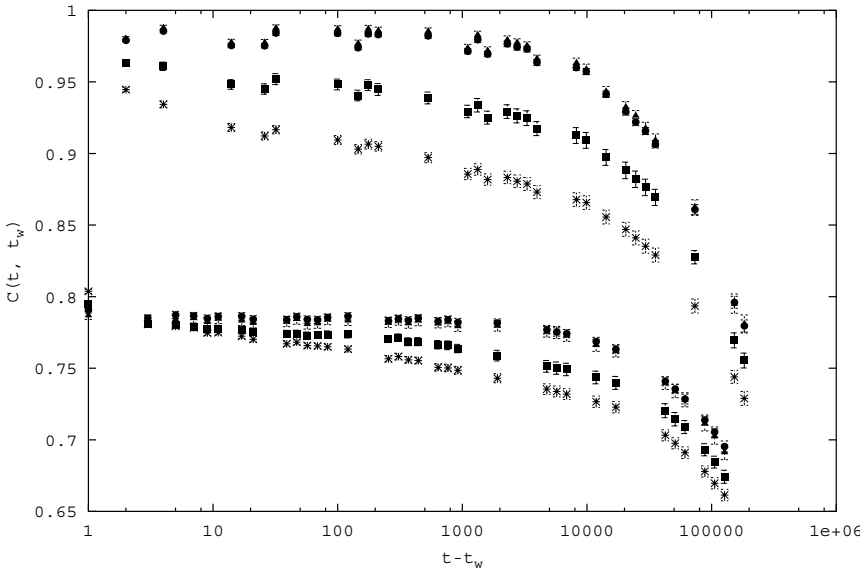

Fig. 7. $C_{22}(t + t_w; t_w)$ for different waiting times before small perturbations. From bottom to top, $t_w = 100$, 5000, 10 000.

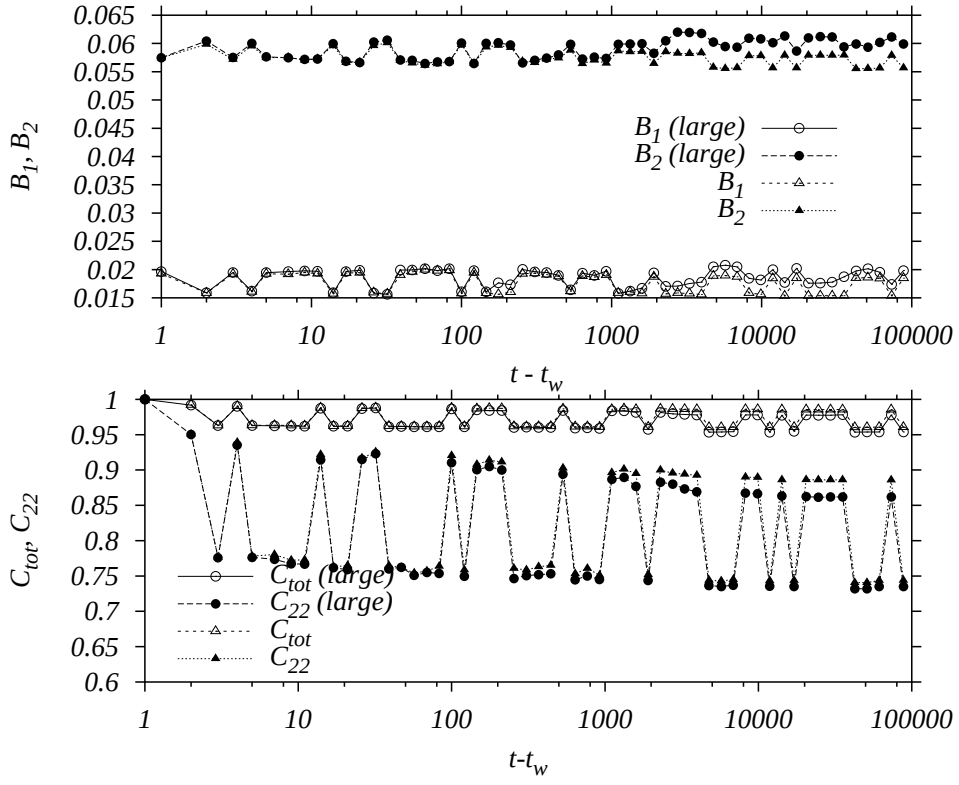

Fig. 8. Densities *vs.* time (upper panel) and autocorrelations *vs.* $t - t_w$ for a system with large immunizations, $L = 50$ and $t_w = 100$. Triangles: without perturbations of any kind. Circles: both large immunizations and small perturbations.

however, this can be understood because the large perturbations are always produced *in the same region*. For very long times the correlations will attain a stationary regime whose active populations contain at least part of the region involved in the immunizations [9]. In other words, the driving produced by the large periodic perturbations is of a completely different nature than that of the small perturbations. The large perturbations seem to play a selective role: the cycles that the system can reach are restricted to those that contain at least part of the populations incorporated during the immunization. According to this picture, the aging effects observed in reference [9] could be simply related to the exploration of the phase space: the older the system the less possibilities of choosing new cycles it would have. In Section 4 we discuss this issue further.

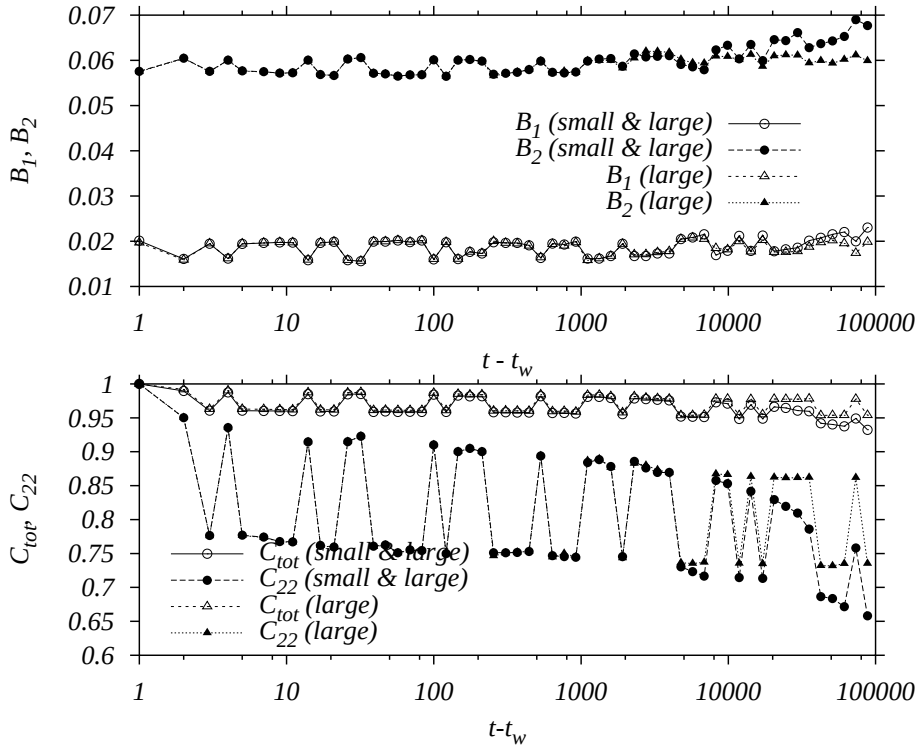

Fig. 9. Densities of active populations *vs.* time (upper panel) and autocorrelations *vs.* $t-t_w$ for $t_w = 100$ and $L = 50$. Triangles: large immunizations only. Circles: both large immunizations and small perturbations.

In Figure 9 we compare the time evolution of the densities B_1 and B_2 and the autocorrelation functions for the system subjected only to large perturbations and for the system with both small perturbations and large immunizations. The results, as expected, confirm the dominance of the small perturbations, over the large ones, in driving the system faster to a different attractor. The increase of the densities around $t \sim 10^4$ for $L = 50$ corresponds to the same finite size effects occurring in Figure 3, being associated to the active populations which have been incorporated into the network by means of the immunization protocol.

4 Concluding remarks

We have analyzed the dynamics of a cellular automata model for the B-cell repertoire which has reproduced experimental results of immunizations on mice. Our analyses provide a broader context in which memory and plasticity take place, as discussed in reference [9].

Defining quantities analogous to the autocorrelation functions used in glassy systems, we have shown that the biologically relevant phenomena takes place in the transient regime of the model. The dependence of these functions on both t and t_w (as opposed to the difference $t-t_w$ only) is reminiscent of the "aging" behavior observed in glassy systems, despite the fact that the underlying dynamics of both systems are controlled by completely different mechanisms.

Starting from different initial conditions the deterministic dynamics takes the system towards a family of long-period attractors. When subjected to random small perturbations (Fig. 4), the system is driven towards a new attractor of the family, revealing that most of the noise is assimilated. However, only part of the large perturbations is incorporated, due to the mechanisms of activation and suppression, leading to a saturation of the learning process [9].

From the biological point of view, the history of the mouse (sample) will be written by the different antigen presentations (random perturbations), starting from its "birth" (initial condition). Since the system is large but finite there is a maximum amount of information it may incorporate. The closer it is to its "destiny" attractor, the less information it is able to learn, since the deeper it already is in a given basin of attraction. Therefore the biological aging corroborated by the experimental results may be simply a consequence of this dynamical feature.

From the results obtained up to now there are evidences that the purely deterministic dynamics is therefore non-ergodic. Despite their large number, however, the family of periodic attractors occupy only a fraction of the phase space. Evidences of this compression in phase space has been obtained in the following computer experiment: selecting randomly two initial configurations (with the same initial concentration), we measured the Hamming distance between them as a function of time as both systems evolve without any perturbation. In Figure 10 we

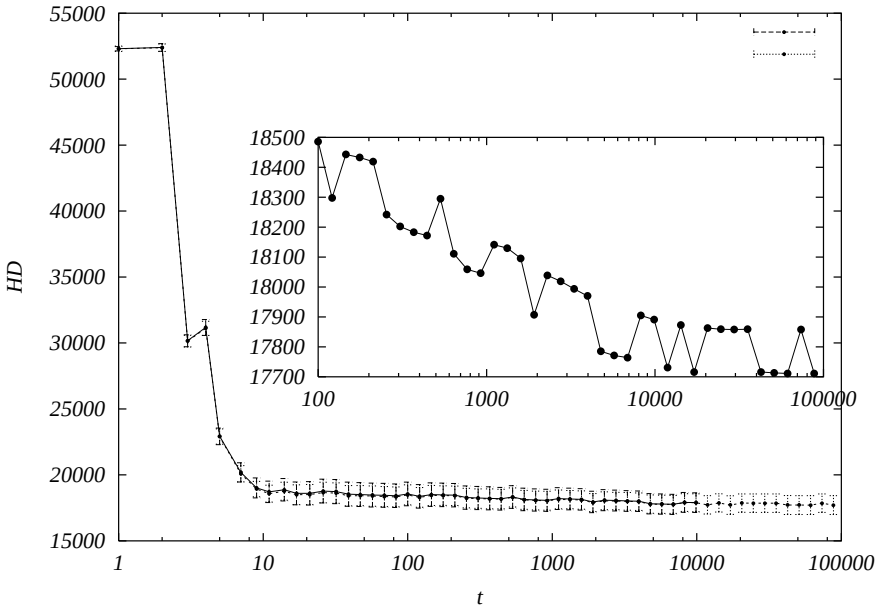

Fig. 10. Hamming distance between 100 pairs of random configurations as a function of time (average and standard deviation). Inset: evolution for $t > 100$ shows that the HD attains a stationary regime for sufficiently long times (standard deviation not shown).

show the evolution of the average HD for 100 pairs (error bars are standard deviations). During the first 10 time steps the HD decreases very rapidly, but for $t > 100$ we observe a quasi-stationary regime, reflecting the slow driving to the attractors (see inset). Note that this behavior is somewhat similar to that of the autocorrelation functions for small t_w.

Still focusing on the evidence of phase space compression, in Figure 11 we present the distribution of HD sampled from $500(500-1)/2$ pairs, for two consecutive time steps ($t = 4000$ and $t = 4001$). The distributions can be well described by a Gaussian, with a width that remains approximately constant (even for long times). Notice that the average value for $t = 4001$ is slightly larger than for $t = 4000$, reflecting the oscillatory behavior of the average HD as the pair of samples reaches their periodic attractors. It should be noted that, for large N, the Central Limit Theorem assures that randomly chosen initial configurations (with the same x) naturally give rise to a Gaussian distribution of the HD between any two of them, at time zero. Interestingly, the CA dynamics does not change the shape of the distribution, its only effect being to essentially shift the Gaussian towards lower mean values, on a long time scale. The spatio-temporal structure of the cycles, as well as their transients and basins of attraction, should be the object of further study and will be published elsewhere.

This work was partially supported by CNPq, Faperj, Finep, Capes and Projeto Enxoval-UFPE. MC and RMZS acknowledge IF-UFF, where part of this work was done during their stay there.

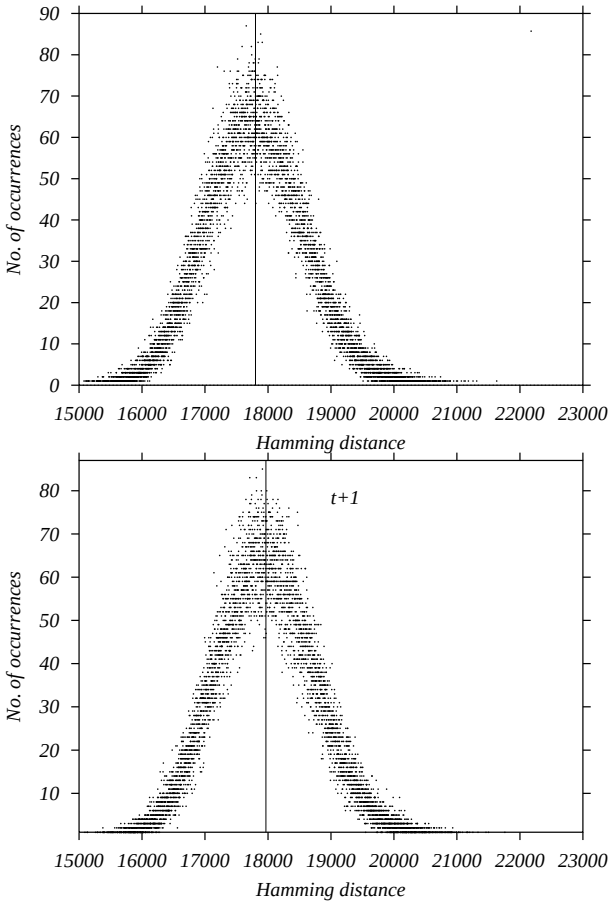

Fig. 11. Distribution of Hamming distance sampled over 500(500-1)/2 configuration pairs at time $t = 4000$ and $t = 4001$. Vertical lines show the average value.

References

1. C.A. Janeway, M.W. Travers, J. Capra, *Imunobiology: The Immune System in Health and Disease*, 4th edn. (Elsevier Science Ltda. Garland Publishing, New York, 2000)
2. N.M. Vaz, A.M.C. de Faria, *Guia Completo de Imunobiologia* (Coopmed Editora, Belo Horizonte, Brazil, 1993)
3. N.K. Jerne, Ann. Immuno. (Inst. Pasteur) C **125**, 373 (1974)
4. D. Holmberg, Å Anderson, L. Carlsson, S. Forsgren, Immunol. Rev. **110**, 84 (1989)
5. A. Coutinho, Immunol. Rev. **110**, 63 (1989)
6. R.M. Zorzenon dos Santos, A.T. Bernardes. Physica A **219**, 1 (1995)
7. A.T. Bernardes, R.M. Zorzenon dos Santos, J. Theor. Biol. **186** 173 (1997)
8. R.M. Zorzenon dos Santos, in Ann. Rev. Comput. Phys. **VI**, 159, edited by D. Stauffer (World Scientific, 1999)
9. R.M. Zorzenon dos Santos, A.T. Bernardes, Phys. Rev. Lett. **81**, 3034 (1998)
10. B. Verdolin, MSc. Thesis, Departamento de Bioquímica e Imunologia, Instituto de Ciências Biológicas, UFMG, Belo Horizonte (1997); A.M.C. Faria *et al.*, Braz. J. Med. Biol. Res. **31**, 35 (1998); N. Vaz *et al.*, Scand. J. Immunol. **46**, 225 (1997)
11. A.M.C. Faria *et al.*, Mech. Ageing Dev. **102**, 67 (1998)
12. W.M. Lahmann, J.S. Menezes, B.A. Verdolin, N.M. Vaz, Braz. J. Med. Biol. Res. **25**, 813 (1992)
13. A.T. Bernardes, R.M. Zorzenon dos Santos, Int. J. Mod. Phys. C **12**, 1 (2001)
14. L.C.E. Struick, *Physical aging in amorphous polymers and other materials* (Elsevier, Houston, 1976)
15. J.-P. Bouchaud, L.F. Cugliandolo, J. Kurchan, M. Mézard, in *Spin Glasses and Random Fields*, edited by A.P. Young (World Scientific, Singapore, 1998)
16. D. Stauffer, G. Weisbuch, Physica A **180**, 42 (1992)
17. R.J. De Boer, L.A. Segel, A.S. Perelson, J. Theor. Biol. **155**, 295 (1992)
18. A.S. Perelson, G.F. Oster, J. Theor. Biol. **81**, 645 (1979)
19. R.M. Zorzenon dos Santos, Physica A **196**, 12 (1993)
20. P.G. Debenedetti, F.H. Stillinger, Nature **410**, 259 (2001)